Published in final edited form as:
J Invest Dermatol. 2010 May ; 130(5): 1227–1236. doi:10.1038/jid.2009.322.

Stem Cells with Neural Crest Characteristics Derived from the Bulge Region of Cultured Human Hair Follicles

Hong Yu[1], **Suresh M. Kumar**[1], **Andrew V. Kossenkov**[2], **Louise Showe**[2], and **Xiaowei Xu**[1]

[1]Department of Pathology and Laboratory Medicine, University of Pennsylvania School of Medicine, Philadelphia, Pennsylvania, USA

[2]The Wistar Institute, Philadelphia, Pennsylvania, USA

Abstract

In this study, we demonstrate that we can isolate stem cells (SCs) with neural crest characteristics from the bulge area of cultured human hair follicles (HFs). These SCs can proliferate in situ and form spheroid structures attached to the bulge area of HFs, and they express immature neural crest cell markers but not differentiation markers. An expression profiling study showed that they share a similar gene expression pattern with murine skin immature neural crest cells. These human SCs are label-retaining cells and are capable of self-renewal through asymmetric cell division *in vitro*. They exhibit clonal multipotency that can give rise to myogenic, melanocytic, and neuronal cell lineages after *in vitro* clonal single cell culture. In addition, these SCs show differentiation potential toward mesenchymal lineages, and they can be differentiated into adipocyte, chondrocyte, and osteocyte lineages. Neuronal differentiation of these cells induces global gene expression changes with a significantly increased expression of neuron-associated genes. Differentiated neuronal cells can persist in mouse brain and retain neuronal differentiation markers. The presence of SCs with neural crest characteristics in HFs may offer new opportunities for the use of these cells in regenerative medicine.

INTRODUCTION

The embryonic neural crest is a population of ectodermally derived precursors that have unique migratory properties and differentiation characteristics. They migrate throughout the body to produce diverse tissue types (Le Douarin and Dupin, 2003; Nagoshi *et al*., 2008). Multipotent/pluripotent cells with characteristics of embryonic neural crest stem cells (NCSCs) have been isolated from several postnatal mouse tissues, including dermis, hair follicles (HFs), and gut (Kruger *et al*., 2002; Fernandes *et al*., 2004; Sieber-Blum *et al*., 2004). Cell fate mapping studies using transgenic mice, which express β-galactosidase in neural crest-derived cells, confirmed that neural crest cells are indeed present in the bulge and dermal papilla of HFs (Wong *et al*., 2006; Nagoshi *et al*., 2008).

Using nestin-driven green fluorescent protein transgenic mice, it has been shown that green fluorescent protein–positive cells are present in the mouse hair bulge, and they are

Correspondence: Xiaowei Xu, Department of Pathology and Laboratory Medicine, University of Pennsylvania School of Medicine, Philadelphia, Pennsylvania 19104, USA. xug@mail.med.upenn.edu.

CONFLICT OF INTEREST

The authors state no conflict of interest.

SUPPLEMENTARY MATERIAL

Supplementary material is linked to the online version of the paper at http://www.nature.com/jid

pluripotent (Amoh *et al*., 2005b; Hoffman, 2006). Mouse epidermal NCSCs (EPI-NCSCs) are present in the bulge of vibrissal follicles, and these stem cells (SCs) can be differentiated into neurons, smooth muscle cells, and Schwann cells under controlled differentiation culture conditions (Sieber-Blum and Grim, 2004; Sieber-Blum *et al*., 2004). Using gene expression profiling, it has been shown that mouse EPI-NCSCs have a signature similar to that of mouse embryonic NCSCs (Hu *et al*., 2006). In addition, neural crest–like SCs have been isolated from dermis; these cells, termed skin-derived precursors (SKPs), express NCSC markers (Fernandes *et al*., 2004; Toma *et al*., 2005; McKenzie *et al*., 2006; Biernaskie *et al*., 2007) and reside in the dermal papilla (Fernandes *et al*., 2004). Therefore, HFs seem to be a niche for murine neural crest–derived SCs.

We, along with others, have shown that SCs with neural crest characteristics can be isolated from human skin and scalp tissue (Belicchi *et al*., 2004; Shih *et al*., 2005; Toma *et al*., 2005; Yu *et al*., 2006); however, these SCs are not well characterized, and the niche for these cells is yet to be defined. In this study, we demonstrate that HF-derived SCs with neural crest characteristics (HFSC/NCC) are located in the bulge region of cultured human HFs. They are label-retaining cells (LRCs) and capable of self-renewal through asymmetric cell division. They have a gene signature similar to that of mouse EPI-NCSCs, and the neuronal cells derived from these SCs may persist in mouse brain and retain the expression of neuronal differentiation markers. These hair-derived SCs may represent a potential new source for regenerative medicine.

RESULTS

Localization of HFSC/NCCs in cultured human HFs

To identify the niche for human HFSC/NCCs, we cultured freshly isolated intact adult and fetal HFs directly in a human embryonic SC culture medium (HESCM4 medium) (Figure 1a, e and h). The outgrowth of these cells from adult HFs can be easily identified in anagen (Figure 1b) or telogen (Figure 1f) HFs after 9 days. Well-formed spheroid structures are present after 3 weeks in anagen (Figure 1c) or telogen (Figure 1g) follicles. The outgrowth is located in the bulge region of anagen or telogen HFs (Figure 1d and g). Fetal HFs have a prominent bulge (Figure 1h), which is visible microscopically and is located just below the sebaceous gland. Well-formed spheres (Figure 1i) composed of compact cells appear ~1 week after culturing fetal HFs in HESCM4 medium. Spheres were found in ~20% of cultured adult or fetal HFs.

To examine the phenotype of the cells in the hair spheres, we fixed HFs with the attached spheres in formalin and processed them for paraffin embedding. Hematoxylin and eosin-stained sections showed that hair spheres are composed of immature cells with a high N/C ratio (Figure 2a). Approximately 30% of cells in the sphere are labeled with Ki67 (Figure 2b), indicating that these cells are in the cell cycle. A majority of cells in the spheres are positive for NCSC markers Twist (Figure 2c), Slug (Figure 2d), and Sox10 (Figure 2e). Interestingly, these cells are also positive for Bmi-1 (Figure 2f) and Notch1 (Figure 2g), which are known to be involved in NCSC self-renewal (Wakamatsu *et al*., 2000; Molofsky *et al*., 2003). These cells are negative for the melanocytic marker S-100 (Figure 2h). The negative control is shown in Figure 2i. Cells in the spheres are negative for a number of other differentiation markers such as microphthalmia-associated transcription factor, neurofilament (NF), cytokeratins (CK20, AE1/3, and PanCK), desmin, c-kit, and collagen type VII (data not shown), indicating that the hair spheres are composed of immature cells expressing immature neural crest cell markers.

Human HFSC/NCCs and mouse EPI-NCSCs have similar gene expression signatures

There are no known stage-specific molecular markers for embryonic NCSCs because the known markers are either expressed by later-stage neural crest–derived cells or in other nonneural crest cell lineages. Hu *et al*. (2006) defined a molecular signature that consists of a panel of 19 genes and is representative of both EPI-NCSC and embryonic NCSC in mouse; Toma *et al*. (2005) also reported a panel of NCSC markers expressed in mouse dermal SKPs. We first compared human HFSC/NCC gene expression with mouse EPI-NCSCs and showed that HFSC/NCCs expressed 18 of 19 genes in the EPI-NCSC signature (Supplementary Table S1). We then compared the gene expression with mouse SKP markers (Fernandes *et al*., 2004; Toma *et al*., 2005) and showed that human HFSC/NCCs express most of the SKP-associated NCSC genes, except *Sca-1* (Supplementary Table S2). Sca-1 is one of the most common markers used to enrich adult murine hematopoietic SCs as well as to distinguish SCs/progenitor cells from other tissues; a human ortholog of Sca-1 has yet to be identified (Holmes and Stanford, 2007). These data suggest that human HFSC/NCCs share a similar genetic signature with mouse EPI-NCSCs and SKPs.

Human HFSC/NCCs are label retaining and capable of self-renewal

To ensure that hair spheres are formed through cell proliferation and not through cell aggregation *in vitro*, we performed a cell mixing study. Hair spheres were dissociated into a single-cell suspension and half the culture was labeled with a tracing dye, carboxyfluorescein diacetate succinimidyl ester (CFDA SE). The labeled cells were then mixed with unlabeled cells. These single cells were then cultured in HESCM4 medium for 1 week and newly formed spheres were examined (Figure 3a). We found that all the spheres were formed by either labeled cells or unlabeled cells (Figure 3b), indicating that the spheres are formed by cell proliferation and not aggregation.

One of the well-known ways to identify SCs is to search for LRCs (Cotsarelis *et al*., 1989, 1990). During the labeling period, BrdU is incorporated into DNA as the cells replicate and is then diluted out of the cellular DNA with each cell cycle during the chase period. Long-term maintenance of BrdU labeling indicates that the cells have a very slow rate of proliferation or exclusive asymmetric division—potential characteristics of SCs. We performed BrdU label-retaining experiments and showed that 12% of the cells retained BrdU labeling after 9 days of *in vitro* chase (Figure 3c), whereas only rare control fibroblasts retained BrdU labeling, indicating that a majority of cells in the HFSC/NCC culture are transit-amplifying cells and a minority are LRCs.

Asymmetric cell division is an important feature of SCs (Roeder and Lorenz, 2006; Ho and Wagner, 2007). To further study whether asymmetric division contributes to label retaining, we examined the distribution of DNA during mitosis in LRCs. We used a cytokinetic inhibitor, nocodazole, to inhibit cytokinesis but not karyokinesis, which resulted in the recovery of many binucleate cells (Roeder and Lorenz, 2006). We exposed BrdU-labeled dissociated hair sphere cells to nocodazole to arrest them during cytokinesis and found that there were indeed many binucleate cells (Figure 3d). We found that BrdU-labeled chromosomes distribute unevenly in binucleate cells. Specifically, BrdU labeling was found exclusively in one daughter nucleus and not in the other (Figure 3e), whereas control fibroblasts showed a symmetric division (data not shown). These data suggest that the label-retaining capacity of human HFSC/NCCs is at least partially due to their asymmetric cell division.

Clonal multipotency and diverse differentiation capacity

We previously showed that human HFSC/NCCs are multi-potent and can be differentiated into myogenic, melanocytic, and neuronal cell lineages (Yu *et al*., 2006). To demonstrate

that a single human HFSC/NCC is multipotent, we performed a limiting dilution assay to isolate clonally derived spheres. Approximately 1% of the seeded dissociated cells were capable of forming a new sphere. Clonally derived spheres were selected randomly from at least three different samples, dissociated and plated in different wells for differentiation assays. Under defined conditions, as described in Materials and Methods, cells from a single human HFSC/NCC were able to form melanocytic (S-100, Figure 4a), neuronal (neural filament, Figure 4b), and smooth muscle (smooth muscle actin, Figure 4c) lineages.

Vertebrate neural crest cells are known to contribute to various structures outside the peripheral nervous system, including the head mesenchyme (Lee *et al*., 2007). We examined human HFSC/NCCs for their capacity to differentiate toward mesenchymal lineages. Early passage HFSC/NCCs were cultured in their respective differentiation media for 7–14 days and examined for specific differentiation marker expression. We showed that differentiated cells express specific markers for adipocytes (oil red staining, Figure 4d) or osteocytes (alkaline phosphate, Figure 4e). In addition, when cultured in chondrocyte differentiation medium for 14 days, ~5% of the cells survived and gained the expression of type II collagen (Figure 4g), indicating that human HFSC/NCCs have the capacity to differentiate into mesenchymal cells. The differentiation efficiency varies depending on target cell type, specifically, 20–40% for melanocytes, adipocytes, and osteocytes; 10% for neurons; 80% for smooth muscle; and 5% for chondrocytes.

Neuronal differentiation and transplantation to mouse brain

Human HFSC/NCCs can be differentiated into neuronal cells *in vitro* (Figure 5a), and the differentiated cells expressed neuron-specific markers such as NF (Figure 5b) and microtubule-associated protein 2 (Figure 5c). To study the global gene expression change after neuronal differentiation, we profiled human HFSC/NCCs before and after neuronal differentiation. We found 1,812 probes with change of twofold or more after differentiation. Gene enrichment analysis was performed for those genes, searching for biological processes or molecular functions that were over-represented in the gene list. Significant enrichments are shown in Table 1. Enriched gene ontology (GO) terms indicate that genes related to the transmission of nerve impulse (GO:0019226), synaptic transmission (GO:0007268), and nervous system development (GO:0007399) are affected by cell differentiation. Genes that significantly (*P*-valueo<0.1) changed by more than twofold are shown in Figure 5g, along with their expression values.

To further characterize the biological behavior of neuronal cells differentiated from HFSC/NCCs *in vivo*, we transplanted them into adult nude mouse brain. Early passage SCs were first differentiated into neuronal cells as previously described (Yu *et al*., 2006) and then labeled with the tracer CFDA SE (Vybrant CFDA SE Cell Tracer Kit; Invitrogen, Carlsbad, CA). Labeled cells were injected unilaterally and stereotactically targeted to the subventricular zone in four nude mice using a Hamilton microsyringe (1×10^5 cells in 3 μl of phosphate-buffered saline). The mice with implants were killed 28 days later. No behavioral changes were observed in these mice. Brains were removed and sectioned for histology and immunohistochemistry for NF. Dye-labeled human cells (green) were present in all four injected mice; however, only a small number of cells survived. Multiple brain sections from the injected site were examined (20 sections per mouse), and the numbers of surviving human cells were 100–150 per mouse in these sections. Most of these cells were located near the needle track (Figure 5d). Some human cells showed an axon-like structure (Figure 5e). A majority of the dye-labeled human cells were positive for NF staining (Figure 5f), suggesting that the differentiated human HFSC/NCCs retain a neuronal phenotype *in vivo*.

HFSC/NCCs in tissue sections

To identify HFSC/NCCs in human HFs *in vivo*, we performed immunohistochemical staining of NCSC markers such as Slug, Twist, and Sox10, as well as double stains of cytokeratin 15 and p75 on human scalp tissues. However, these proposed neural crest markers are not specific for neural crest lineages in the skin. Subpopulations of keratinocytes in HFs and mesenchymal cells in the dermis were also positive (data not shown), and we were unable to definitively identify HFSC/NCCs *in situ* in HFs using this approach.

DISCUSSION

Hair follicles undergo lifelong cyclic proliferation and regression, and the bulge provides a unique differentiation-restricted environment for different types of adult SCs (Cotsarelis *et al*., 1989, 1990; Morris *et al*., 2004). Epithelial and melanocyte SCs are known to be in the bulge area; we now show that HFSC/NCCs are also located in the bulge region of cultured human HFs.

Mouse EPI-NCSCs have been demonstrated in vibrissa HFs (Sieber-Blum and Grim, 2004; Sieber-Blum *et al*., 2004). However, major differences exist between rodent and human HFs (Cotsarelis, 2006). For example, human scalp follicles are significantly larger, reaching lengths of 5 mm, compared with mouse pelage follicles, which are only 1 mm long. Rodent vibrissa (whisker) follicles are larger than pelage follicles but are highly unusual in their structure and hair-cycling capabilities. Another difference is that human HFs grow for years rather than weeks in rodents. Thus, the cellular and molecular characteristics of adult SCs in human HFs can be quite different from those in rodents. Indeed, it has been shown that mouse nestin-positive bulge SCs can be differentiated into multiple lineages including cytokeratin 15-positive keratinocytes (Amoh *et al*., 2005b). However, we were unable to differentiate human HFSC/NCCs into keratinocytes, despite multiple trials with various differentiation media (data not shown), suggesting that the differentiation capacities of human and mouse hair-derived SCs are not identical. Nevertheless, we showed that human and mouse hair-derived neural crest-like SCs share similar gene expression signatures. The niche for human SKPs has been shown to be in the dermal papilla (Hunt *et al*., 2008), and we showed that the niche for HFSC/NCCs is in the bulge region of cultured human HFs. Before culturing, we used dispase treatment to separate follicular epithelium from the surrounding mesenchymal tissues, which include dermal papilla and perifollicular fibrous sheath, and histology of the isolated HFs did not show dermal cell contamination (Yu *et al*., 2006). Therefore, it is unlikely that SCs in perifollicular mesenchymal tissues contributed to the spheres in the bulge region seen in our study. Nevertheless, we were unable to definitively identify HFSC/NCCs in HF tissue sections because the proposed neural crest markers, such as Slug, Twist, and p75, are not specific for neural crest lineages in the skin. Therefore, the origin of these sphere-forming cells in the HF, including the possibility of reprogramming, remains to be investigated.

Quiescent SCs can generally be identified as LRCs that retain BrdU over a long period (Bickenbach and Mackenzie, 1984). This approach has been used to identify SCs in the bulge region of the HF, in the limbus of the cornea, and in crypts of intestine, and it is considered the gold standard for epithelial SC identification (Cotsarelis *et al*., 1989, 1990; Scoville *et al*., 2008). LRCs are likely to result from an asymmetric division of adult SCs (Roeder and Lorenz, 2006; Ho and Wagner, 2007), during which the SCs simultaneously generate identical copies of themselves but also give rise to a more differentiated progenitor of transit-amplifying cells. We showed that HFSC/NCCs divided in the culture medium by asymmetric division and that 12% of the cells can retain BrdU labeling, indicating that the

HFSC/NCC culture is a mixture of SCs and transit-amplifying cells and suggesting that label-retaining HFSC/NCCs are capable of self-renewal.

Pluripotent NCSCs have been isolated from hair and skin and successfully used for cell-replacement therapy in rodents (Amoh *et al*., 2009). Hoffman and colleagues showed that nestin-positive bulge SCs can be used to facilitate the healing of severed sciatic nerves and spinal cord (Amoh *et al*., 2005a, 2008). Sieber-Blum *et al*. (2006) reported that when EPI-NCSCs were grafted into mouse spinal cord, they survived, integrated, and intermingled with host neurites. McKenzie *et al*. (2006) showed that SKPs can generate Schwann cells that myelinate central nervous system axons when transplanted into the dysmyelinated brain of neonatal shiverer mice. More recently, they showed that 12 weeks after transplantation of SKPs within the injured spinal cord, these cells provided a bridge across the lesion site, increased the size of the spared tissue rim, myelinated spared axons within the tissue rim, reduced reactive gliosis, and provided an environment that was highly conducive to axonal growth; moreover, SKPs provide enhanced locomotor recovery (Biernaskie *et al*., 2007). We showed that human HFSC/NCCs in HFs have gene expression signatures similar to those of these murine neural crest cells, and neuronal cells derived from human HFSC/NCCs can survive and retain neuronal differentiation *in vivo* in mouse brain. These results suggest that human HFSC/NCCs may have functions similar to those of murine skin NCSCs. Further studies are necessary to investigate whether they are a potential autologous source of cells for transplantation to treat injured spinal cord or nerve.

MATERIALS AND METHODS

Isolation of human HFSC/NCCs from HFs

Hair follicles were isolated from 15 fetal scalp tissues (22–24 weeks) and from 10 adult patients (50–65 years) obtained through Advanced Bioscience Resources (Alameda, CA) and the Cooperative Human Tissue Network (CHTN), with approval from the Institutional Review Board of the University of Pennsylvania. HFs were isolated as described previously (Xu *et al*., 2003; Roh *et al*., 2004, 2005). Briefly, tissues were rinsed, trimmed to remove excess adipose tissue, cut into small pieces, and subjected to enzymatic dissociation in 4.8 mg ml^{-1} dispase (Invitrogen) in DMEM at 4 °C overnight. For adult samples, after treatment, the epidermis was peeled off from the dermis, and HFs were plucked from the dermis. For fetal scalp, hair with epidermis was scraped off from the dermis with a scalpel and was then treated with 0.5% collagenase containing 5% fetal bovine serum for 30 minutes at room temperature. HFs were collected and washed with phosphate-buffered saline. To obtain viable single cells from follicular epithelium, HFs were treated twice with 0.25% trypsin/EDTA (Invitrogen) for 30 minutes at 37 °C. The cell suspension was filtered through a 40-μm cell strainer (BD Falcon, Bedford, MA), and the cells were counted. Single cells were cultured in uncoated flasks containing conditioned HESC medium supplemented with additional basic fibroblast growth factor at 4 ng ml^{-1} (HESCM4 medium) before use (Thomson *et al*., 1998; Zhang *et al*., 2001). Keratinocytes gradually die in the medium, whereas HFSC/NCCs can proliferate as attached cells or spheres. To study the niche for HFSC/NCCs, we cultured HFs directly in the HESCM4 medium. These HFs were followed daily for 3 weeks. HFs with attached spheres were fixed in 10% formalin and processed for paraffin embedding for histology and immunohistochemistry.

Immunocytochemistry and immunohistochemistry

Cultured cells were fixed with 4% paraformaldehyde and stained with primary antibodies specific for microtubule-associated protein-2 (Sigma, St Louis, MO), HMB45/SILV (DakoCytomation, Carpinteria, CA), NF-M (a gift from Virginia Lee), and smooth muscle actin (Chemicon, Temecula, CA). Isotype-matched mouse antibodies or normal rabbit IgG

were used as controls. After washing, primary antibody binding was detected using corresponding goat anti-mouse or anti-rabbit Alexa Fluor 488-conjugated or donkey anti-goat Alexa Fluor 594 secondary antibodies (1:600–1:1,000; Invitrogen). Cells were counterstained with either 4-diamidino-2-phenylindole (DAPI) (Invitrogen) or TO-PRO-3 (Invitrogen) to show nuclei. Staining was observed through a Nikon E600 upright fluorescence microscope or Leica TCS SP2 microscope. Formalin-fixed, paraffin-embedded tissues were used for hematoxylin and eosin, Sox10, Ki67, Slug, Twist, tyrosinase, Bmi-1, Notch1, NF, c-kit, and pan-cytokeratin staining as previously described (Yu *et al*., 2006), following standard protocols.

Cell mixing, label retaining, and asymmetric cell division assays

Hair spheres were harvested and dissociated into single-cell suspensions. Half of the cells were labeled with the tracing dye CFDA SE (Vybrant CFDA SE Cell Tracer Kit; Invitrogen) as recommended by the manufacturer. Briefly, cells were incubated in 10 μM dye at 37 °C for 15 min and transferred to a fresh culture medium for 30 min at 37 °C. Labeled cells were washed, harvested, and counted and then mixed equally with unlabeled cells. The single-cell mixture was then cultured in HESCM4 medium for 1 week and newly formed spheres were examined under a fluorescence microscope.

One of the well-known ways to identify SCs is to search for LRCs (Cotsarelis *et al*., 1989, 1990). To identify LRCs, dissociated hair sphere cells were replated in HESCM4 medium, pulse labeled with BrdU (0.6 μM) for 48 hours using a BrdU labeling and staining kit (Chemicon), washed with Dulbecco's phosphate-buffered saline, and then allowed to grow in the same medium for an additional 9 days. The cells were fixed and stained with anti-BrdU (mouse monoclonal, 1:100, Sigma) and goat anti-mouse Alexa Fluor 488-conjugated secondary antibody.

Asymmetric cell division is an important feature of SCs (Roeder and Lorenz, 2006; Ho and Wagner, 2007). We examined whether HFSC/NCCs distribute DNA asymmetrically. We used a cytokinetic inhibitor, nocodazole, to inhibit cytokinesis but not karyokinesis, which resulted in the recovery of many binucleate cells (Roeder and Lorenz, 2006). We exposed BrdU-labeled dissociated hair sphere cells to 0.1 μg ml^{-1} nocodazole for 16 hours to arrest them during cytokinesis. The cells were fixed and BrdU was visualized as described above.

Differentiation assays

Hair spheres and attached cells were enzymatically dissociated into single cells before being plated onto tissue culture–grade plastic coated with 10 ng ml^{-1} fibronectin (melanogenic, smooth muscle, adipogenic, osteogenic, and chondrogenic differentiation) or 0.1% Matrigel (BD Biosciences, San Jose, CA; neuronal differentiation) in differentiation medium. Melanocytic, smooth muscle, and neuronal differentiation was carried out as previously described (Yu *et al*., 2006). Adipogenesis was induced in differentiation medium containing 90% low-glucose DMEM, 1 insulin-transferrin-sodium selenite medium supplement, 1 mg ml^{-1} linoleic acid-bovine serum albumin, 1 μM hydrocortisone, 60 μM indomethacin, 0.5 μM isobutylmethylxanthine, and 10% horse serum and evaluated by Oil Red O adipogenic staining. Osteogenesis was induced in differentiation medium containing 90% low-glucose DMEM, 1 × insulin-transferrin-sodium selenite medium supplement, 1 mg ml^{-1} linoleic acid-bovine serum albumin, 0.1 μM dexamethasone, 0.05 M L-ascorbic acid 2-phosphate, 10 μM α-glycerophosphate, and 10% fetal calf serum and evaluated by alkaline phosphatase histochemical staining. Chondrogenesis was induced in medium containing 90% DMEM, 1 × insulin-transferrin-sodium selenite medium supplement, 1 mg ml^{-1} linoleic acid-bovine serum albumin, 0.05 μM dexamethasone, 10 ng ml^{-1} transforming growth factor-β1, and 1 μM pyruvate and evaluated by type II collagen chondrogenic immunostaining.

Limiting dilution assay

Dissociated individual cells from hair spheres were serially diluted in HESCM4 medium in uncoated 96-well plates. Each well was assessed microscopically for the presence of a single cell. Wells containing no cells or more than one cell were excluded. The clonally derived spheres were dissociated and plated in different wells for differentiation assays.

Transplantation of differentiated cells

Early-passage human HFSC/NCCs were expanded in HESCM4 medium and then cultured in neuronal differentiation medium for 21 days as previously described. These cells were labeled with tracer CFDA SE (Vybrant CFDA SE Cell Tracer Kit; Invitrogen). The labeled cells were then injected unilaterally and stereotactically targeted to the subventricular zone in four nude mice using a Hamilton microsyringe (1×10^5 cells in 3 μl of phosphate-buffered saline). The mice with implants were killed 28 days later. No behavioral changes were observed in these mice. The brains were removed, equilibrated in 30% sucrose, embedded in cryoembedding compound, frozen, and cut into 10 μm-thick cross-sections for histology and immunohistochemistry for human-specific NF. Some sections were counterstained with 25 ng ml^{-1} DAPI to visualize nuclei. Implanted human cells were counted and photographed using a fluorescence microscope (single fluorescein tube or triple tube with fluorescein, Texas red, and DAPI optics). Rat anti-NF antibody was used to detect NF expression, which was visualized using a chick anti-rat secondary antibody labeled with Alexa Fluor 594.

Gene expression profiling and data analysis

For gene expression profiling, mRNA from early passage human HFSC/NCCs before and after neuronal differentiation (two pairs) was hybridized on Affy HG-U133 Plus 2.0 arrays (Affimetrix, Santa Clara, CA) at the University of Pennsylvania microarray facility. Data were normalized using quantile normalization. Probes that were not significantly expressed above the background level in all four samples were removed, resulting in 29,202 probes taken for further analysis. Fold changes were calculated as the ratio of the average expression of differentiated samples to the average expression of undifferentiated samples. Significance of the fold change difference was estimated using an unpaired two-sided *t*-test. Gene enrichment analysis was carried out on the list of probes with a fold change of two or more using DAVID software (National Institute of Allergy and Infectious Diseases, Bethesda, MD) (Sherman *et al*., 2007) only for the GO biological process and molecular function categories. Term enrichments with Bonferroni corrected *P*-values <0.1 and more than 20 gene hits were called significant.

Heatmaps for gene expression were plotted along with two-way hierarchical clustering using Pearson's correlation distance for genes and normalized Euclidean distance for samples. Color coding indicates the fold change difference between the corresponding expression value of the gene in the sample and the average expression across all samples for the gene. For gene expression signature comparison, a marker with a detection *P*-value<0.05 in at least one sample (as determined by MAS 5.0 Affymetrix software, Affimetrix, Santa Clara, CA) was defined as expressed in our experiment. Fold changes were calculated relative to the average background level of a microarray chip.

Statistical analysis

For the label-retaining experiment, statistical analysis was performed using a two-tailed Student's *t*-test; $P<0.05$ was considered significant.

Supplementary Material

Refer to Web version on PubMed Central for supplementary material.

Acknowledgments

We are grateful to M Herlyn for advice and V Lee for providing the NF antibody. This study was supported by AR054593 and by the University Research Foundation from the University of Pennsylvania to X Xu.

Abbreviations

CFDA SE	carboxyfluorescein diacetate succinimidyl ester
EPI-NCSC	epidermal neural crest stem cell
HF	hair follicle
HFSC/NCC	hair follicle–derived stem cell with neural crest characteristics
LRC	label-retaining cell
NCSC	neural crest stem cell
NF	neurofilament
SC	stem cell
SKP	skin-derived precursor

REFERENCES

Amoh Y, Kanoh M, Niiyama S, Kawahara K, Sato Y, Katsuoka K, et al. Human and mouse hair follicles contain both multipotent and monopotent stem cells. Cell Cycle 2009;8:176–7. [PubMed: 19106614]

Amoh Y, Li L, Campillo R, Kawahara K, Katsuoka K, Penman S, et al. Implanted hair follicle stem cells form Schwann cells that support repair of severed peripheral nerves. Proc Natl Acad Sci USA 2005a;102:17734–8. [PubMed: 16314569]

Amoh Y, Li L, Katsuoka K, Hoffman RM. Multipotent hair follicle stem cells promote repair of spinal cord injury and recovery of walking function. Cell Cycle 2008;7:1865–9. [PubMed: 18583926]

Amoh Y, Li L, Katsuoka K, Penman S, Hoffman RM. Multipotent nestin-positive, keratin-negative hair-follicle bulge stem cells can form neurons. Proc Natl Acad Sci USA 2005b;102:5530–4. [PubMed: 15802470]

Belicchi M, Pisati F, Lopa R, Porretti L, Fortunato F, Sironi M, et al. Human skin-derived stem cells migrate throughout forebrain and differentiate into astrocytes after injection into adult mouse brain. J Neurosci Res 2004;77:475–86. [PubMed: 15264217]

Bickenbach JR, Mackenzie IC. Identification and localization of label-retaining cells in hamster epithelia. J Invest Dermatol 1984;82:618–22. [PubMed: 6725984]

Biernaskie J, Sparling JS, Liu J, Shannon CP, Plemel JR, Xie Y, et al. Skin-derived precursors generate myelinating Schwann cells that promote remyelination and functional recovery after contusion spinal cord injury. J Neurosci 2007;27:9545–59. [PubMed: 17804616]

Cotsarelis G. Gene expression profiling gets to the root of human hair follicle stem cells. J Clin Invest 2006;116:19–22. [PubMed: 16395398]

Cotsarelis G, Cheng SZ, Dong G, Sun TT, Lavker RM. Existence of slow-cycling limbal epithelial basal cells that can be preferentially stimulated to proliferate: implications on epithelial stem cells. Cell 1989;57:201–9. [PubMed: 2702690]

Cotsarelis G, Sun TT, Lavker RM. Label-retaining cells reside in the bulge area of pilosebaceous unit: implications for follicular stem cells, hair cycle, and skin carcinogenesis. Cell 1990;61:1329–37. [PubMed: 2364430]

Fernandes KJ, McKenzie IA, Mill P, Smith KM, Akhavan M, Barnabe-Heider F, et al. A dermal niche for multipotent adult skin-derived precursor cells. Nat Cell Biol 2004;6:1082–93. [PubMed: 15517002]

Ho AD, Wagner W. The beauty of asymmetry: asymmetric divisions and self-renewal in the haematopoietic system. Curr Opin Hematol 2007;14:330–6. [PubMed: 17534157]

Hoffman RM. The pluripotency of hair follicle stem cells. Cell Cycle 2006;5:232–3. [PubMed: 16410728]

Holmes C, Stanford WL. Concise review: stem cell antigen-1: expression, function, and enigma. Stem Cells 2007;25:1339–47. [PubMed: 17379763]

Hu YF, Zhang ZJ, Sieber-Blum M. An epidermal neural crest stem cell (EPI-NCSC) molecular signature. Stem Cells 2006;24:2692–702. [PubMed: 16931771]

Hunt DP, Morris PN, Sterling J, Anderson JA, Joannides A, Jahoda C, et al. A highly enriched niche of precursor cells with neuronal and glial potential within the hair follicle dermal papilla of adult skin. Stem Cells 2008;26:163–72. [PubMed: 17901404]

Kruger GM, Mosher JT, Bixby S, Joseph N, Iwashita T, Morrison SJ. Neural crest stem cells persist in the adult gut but undergo changes in self-renewal, neuronal subtype potential, and factor responsiveness. Neuron 2002;35:657–69. [PubMed: 12194866]

Le Douarin NM, Dupin E. Multipotentiality of the neural crest. Curr Opin Genet Dev 2003;13:529–36. [PubMed: 14550420]

Lee G, Kim H, Elkabetz Y, Al SG, Panagiotakos G, Barberi T, et al. Isolation and directed differentiation of neural crest stem cells derived from human embryonic stem cells. Nat Biotechnol 2007;25:1468–75. [PubMed: 18037878]

McKenzie IA, Biernaskie J, Toma JG, Midha R, Miller FD. Skin-derived precursors generate myelinating Schwann cells for the injured and dysmyelinated nervous system. J Neurosci 2006;26:6651–60. [PubMed: 16775154]

Molofsky AV, Pardal R, Iwashita T, Park IK, Clarke MF, Morrison SJ. Bmi-1 dependence distinguishes neural stem cell self-renewal from progenitor proliferation. Nature 2003;425:962–7. [PubMed: 14574365]

Morris RJ, Liu Y, Marles L, Yang Z, Trempus C, Li S, et al. Capturing and profiling adult hair follicle stem cells. Nat Biotechnol 2004;22:411–7. [PubMed: 15024388]

Nagoshi N, Shibata S, Kubota Y, Nakamura M, Nagai Y, Satoh E, et al. Ontogeny and multipotency of neural crest-derived stem cells in mouse bone marrow, dorsal root ganglia, and whisker pad. Cell Stem Cell 2008;2:392–403. [PubMed: 18397758]

Roeder I, Lorenz R. Asymmetry of stem cell fate and the potential impact of the niche: observations, simulations, and interpretations. Stem Cell Rev 2006;2:171–80. [PubMed: 17625253]

Roh C, Tao Q, Lyle S. Dermal papilla-induced hair differentiation of adult epithelial stem cells from human skin. Physiol Genomics 2004;19:207–17. [PubMed: 15292489]

Roh C, Tao Q, Photopoulos C, Lyle S. *In vitro* differences between keratinocyte stem cells and transit-amplifying cells of the human hair follicle. J Invest Dermatol 2005;125:1099–105. [PubMed: 16354178]

Scoville DH, Sato T, He XC, Li L. Current view: intestinal stem cells and signaling. Gastroenterology 2008;134:849–64. [PubMed: 18325394]

Sherman BT, Huang dW, Tan Q, Guo Y, Bour S, Liu D, et al. DAVID Knowledgebase: a gene-centered database integrating heterogeneous gene annotation resources to facilitate high-throughput gene functional analysis. BMC Bioinformatics 2007;8:426. [PubMed: 17980028]

Shih DT, Lee DC, Chen SC, Tsai RY, Huang CT, Tsai CC, et al. Isolation and characterization of neurogenic mesenchymal stem cells in human scalp tissue. Stem Cells 2005;23:1012–20. [PubMed: 15941858]

Sieber-Blum M, Grim M. The adult hair follicle: cradle for pluripotent neural crest stem cells. Birth Defects Res C Embryo Today 2004;72:162–72. [PubMed: 15269890]

Sieber-Blum M, Grim M, Hu YF, Szeder V. Pluripotent neural crest stem cells in the adult hair follicle. Dev Dyn 2004;231:258–69. [PubMed: 15366003]

Sieber-Blum M, Schnell L, Grim M, Hu YF, Schneider R, Schwab ME. Characterization of epidermal neural crest stem cell (EPI-NCSC) grafts in the lesioned spinal cord. Mol Cell Neurosci 2006;32:67–81. [PubMed: 16626970]

Thomson JA, Itskovitz-Eldor J, Shapiro SS, Waknitz MA, Swiergiel JJ, Marshall VS, et al. Embryonic stem cell lines derived from human blastocysts. Science 1998;282:1145–7. [PubMed: 9804556]

Toma JG, McKenzie IA, Bagli D, Miller FD. Isolation and characterization of multipotent skin-derived precursors from human skin. Stem Cells 2005;23:727–37. [PubMed: 15917469]

Wakamatsu Y, Maynard TM, Weston JA. Fate determination of neural crest cells by NOTCH-mediated lateral inhibition and asymmetrical cell division during gangliogenesis. Development 2000;127:2811–21. [PubMed: 10851127]

Wong CE, Paratore C, Dours-Zimmermann MT, Rochat A, Pietri T, Suter U, et al. Neural crest-derived cells with stem cell features can be traced back to multiple lineages in the adult skin. J Cell Biol 2006;175:1005–15. [PubMed: 17158956]

Xu X, Lyle S, Liu Y, Solky B, Cotsarelis G. Differential expression of cyclin D1 in the human hair follicle. Am J Pathol 2003;163:969–78. [PubMed: 12937137]

Yu H, Fang D, Kumar SM, Li L, Nguyen TK, Acs G, et al. Isolation of a novel population of multipotent adult stem cells from human hair follicles. Am J Pathol 2006;168:1879–88. [PubMed: 16723703]

Zhang SC, Wernig M, Duncan ID, Brustle O, Thomson JA. *In vitro* differentiation of transplantable neural precursors from human embryonic stem cells. Nat Biotechnol 2001;19:1129–33. [PubMed: 11731781]

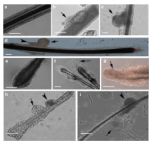

Figure 1. Sphere formation in the bulge region of cultured follicles

(**a**) A freshly plucked adult anagen hair follicle before culture. (**b**) An adult anagen hair follicle was cultured for 9 days, with some cells starting to grow out (arrow). (**c**) An adult anagen hair follicle was cultured for 3 weeks. A well-formed sphere can be seen (arrow). (**d**) View of an entire adult anagen hair; the sphere is located in the bulge area (arrow), below the portion of the sebaceous gland (arrowhead). (**e**) A freshly plucked adult telogen hair follicle before culture. (**f**) Adult telogen hair follicles were cultured for 9 days, with some cells starting to grow out (arrows). (**g**) A telogen hair follicle was cultured for 3 weeks. A well-formed sphere composed of compact cells can be seen (arrow). (**h**) A freshly isolated fetal anagen hair follicle with a prominent bulge (arrow), which is located below the sebaceous gland (arrowhead). (**i**) A fetal anagen hair follicle was cultured for ~1 week. A well-formed sphere composed of compact cells can be seen (arrow) just below the sebaceous gland (arrowhead). Bars = 1 mm.

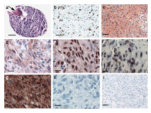

Figure 2. Characterization of spheres derived from the bulge region of cultured follicles

Sections of paraffin-embedded hair spheres were stained with hematoxylin and eosin, or immunohistochemistry (IHC) was carried out with various antibodies. (**a**) A hair sphere is composed of immature cells with a high N/C ratio (hematoxylin and eosin, arrow points to hair shaft). (**b**) About 30% of cells are positive for Ki67 (Ki67 shows nuclear stain pattern). (**c**) A majority of hair sphere cells are positive for Twist (Twist shows nuclear stain pattern). (**d**) A majority of hair sphere cells are positive for Slug (Slug shows nuclear stain pattern). (**e**) A majority of hair sphere cells are positive for Sox10 (Sox10 shows nuclear stain pattern). (**f**) A majority of hair sphere cells are positive for Bmi-1 (Bmi-1 shows nuclear stain pattern). (**g**) A majority of hair sphere cells are positive for Notch1 (Notch1 shows both cytoplasmic and nuclear stain pattern). (**h**) Hair sphere cells are negative for S-100 staining (S-100 stain). (**i**) Representative image for isotype negative control for IHC. Bars in a, b, c, i = 30 μM, Bars in d–h = 10 μM.

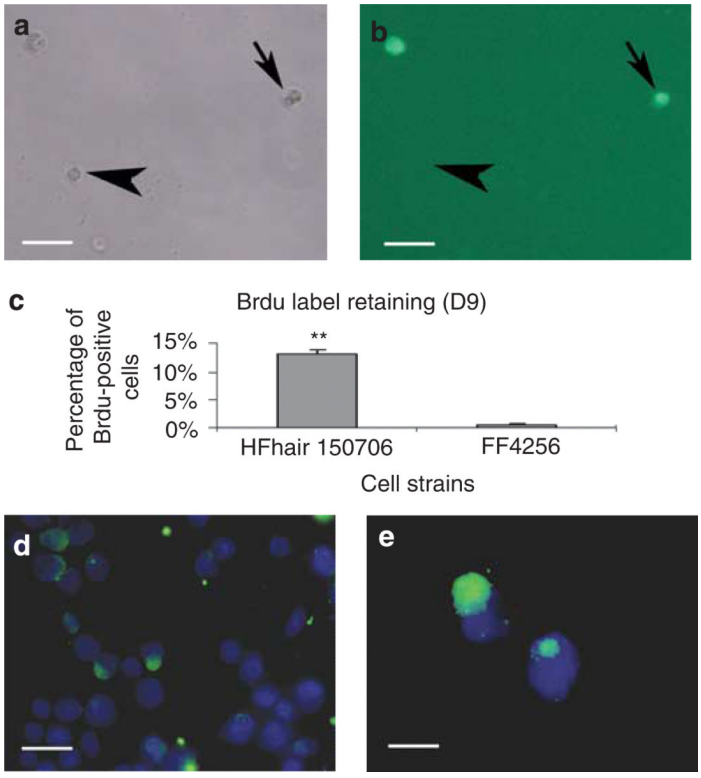

Figure 3. Growth characteristics of human hair follicle–derived stem cell with neural crest characteristics (HFSC/NCCs)

(**a–b**) Cell mixing study. Carboxyfluorescein diacetate succinimidyl ester (CFDA SE)–labeled and unlabeled HFSC/NCCs were mixed together and cultured for 1 week. Small spheres composed of several cells can be seen under differential interference contrast microscopy in **a**. Either all or none of the cells within the hair sphere were fluorescent (**b**). Arrows point to CFDA SE–positive cells; arrowheads point to CFDA SE–negative cells showing weak autofluorescence. (**c**) BrdU label retaining. After 9 days of chase, 12% of HFSC/NCCs are label-retaining cells (LRCs), whereas only rare positive cells are in fibroblasts. A double asterisk (**) indicates $P<0.001$. (**d–e**) Asymmetric cell division. Human HFSC/NCCs were labeled with BrdU and then treated with nocodazole. There were binucleate cells (**d**). Only one daughter cell retained BrdU labeling with green fluorescence (**e**), indicating an asymmetric division. Nuclei were visualized with Hoechst 33258 (blue). Bars in a, b = 75 μM. Bar in d = 15 μM; Bar in 7.5 μM.

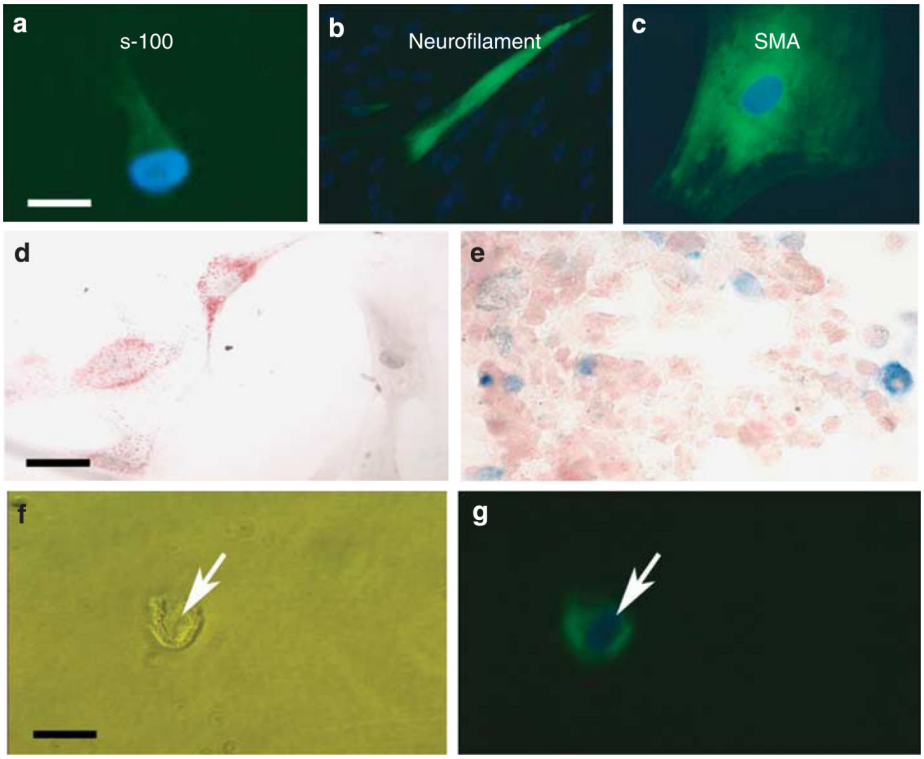

Figure 4. Differentiation capacity of human hair follicle–derived stem cell with neural crest characteristics (HFSC/NCCs)

(**a–c**) Multipotency of a single HFSC/NCC. A single cell–derived colony was able to differentiate into melanocytes (**a**, S-100 staining), neurons (**b**, neural filament staining), and smooth muscle cells (**c**, SMA staining). (**d**) Adipocyte differentiation. Oil red staining shows oil droplets in the cytoplasm of differentiated cells. (**e**) Osteocyte differentiation. Alkaline phosphatase staining shows a number of positive cells. (**f** and **g**) Chondrocyte differentiation. Differential interference contrast image of a cell after differentiation is shown in **f**. Type II collagen staining was visualized with a fluorescein-labeled secondary antibody, and the nucleus was stained with 4-diamidino-2-phenylindole. The differentiated cells are positive for type II collagen in **g**, a marker for chondrocytes (arrow points to a nucleus). Bars = 10 μM.

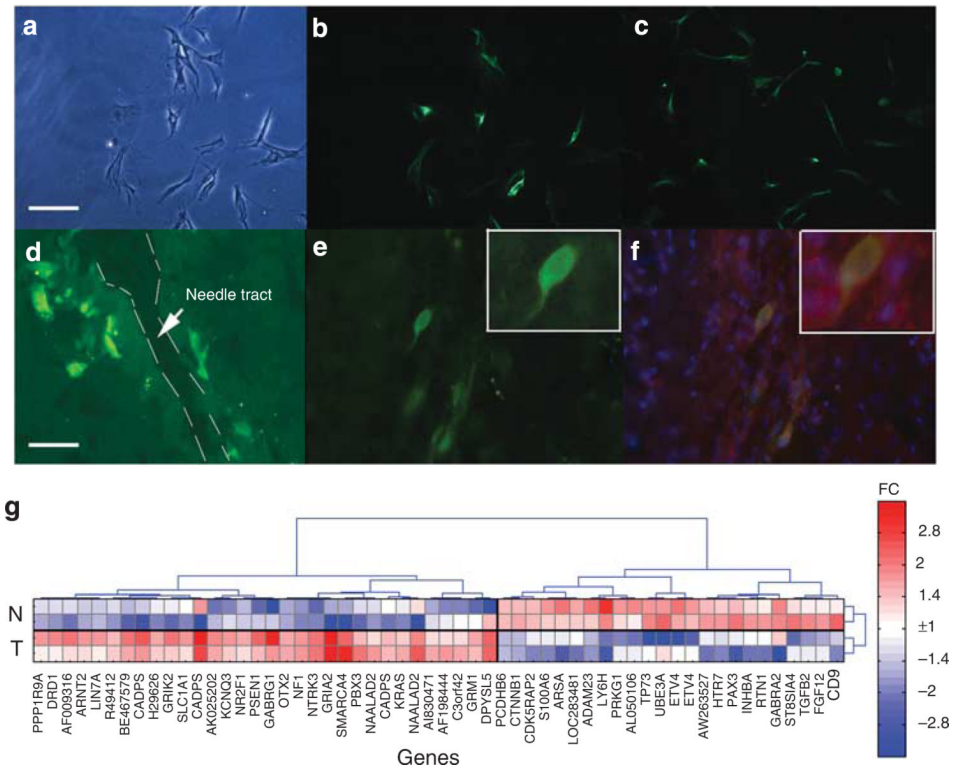

Figure 5. Transplantation of human hair follicle–derived stem cell with neural crest characteristics (HFSC/NCCs) *in vivo*

(**a–c**) Neuronal differentiation of HFSC/NCCs in culture. (**a**) Differential interference contrast image; (**b**) neurofilament (NF) staining; (**c**) microtubule-associated protein 2 (MAP2) staining. (**d**) Frozen sections of mouse brain near the needle injection site (fluorescein tube). Cells with green fluorescence, adjacent to the needle tract, are human cells labeled with carboxyfluorescein diacetate succinimidyl ester (CFDA SE). (**e**) One cell in the center shows an axon-like structure (fluorescein tube). This cell was enlarged and is shown in the right upper corner. (**f**) The same area after NF staining; a few human cells were positive for both CFDA SE and NF stains, suggesting that HFSC/NCCs retain at least some neuron phenotypes *in vivo* (fluorescein, Texas red, and DAPI triple tube). One positive cell was enlarged and is shown in the upper right corner. (**g**) Expression values for 56 differentially expressed genes (fold change >2, *P*-valueo<0.1) that are involved in nervous system–related processes. N, nondifferentiated samples; T, differentiated samples; FC, fold change from average expression.

Table 1

GO term enrichment in the list of differentially expressed genes

GO term	Type	Enr	*n*	% Of total	*P*-value	*P*-value (Bonf.)
GO:0007398: ectoderm development	BP	3.66	35	22%	6×10^{-11}	3×10^{-7}
GO:0008544: epidermis development	BP	3.48	31	21%	3×10^{-9}	2×10^{-5}
GO:0048514: blood vessel morphogenesis	BP	2.90	29	17%	6×10^{-7}	0.003
GO:0001568: blood vessel development	BP	2.83	32	17%	3×10^{-7}	0.001
GO:0009888: tissue development	BP	2.80	57	17%	4×10^{-12}	2×10^{-8}
GO:0001525: angiogenesis	BP	2.79	24	17%	10^{-5}	0.07
GO:0001944: vasculature development	BP	2.79	32	17%	4×10^{-7}	0.002
GO:0001501: skeletal development	BP	2.41	33	14%	6×10^{-6}	0.003
GO:0009887: organ morphogenesis	BP	2.32	58	14%	4×10^{-9}	2×10^{-5}
GO:0051239: regulation of multicellular organismal process	BP	2.28	40	14%	2×10^{-6}	0.02
GO:0048513: organ development	BP	2.23	172	13%	10^{-24}	5×10^{-21}
GO:0019226: transmission of nerve impulse	**BP**	**2.20**	**46**	**13%**	$\mathbf{9 \times 10^{-7}}$	**0.005**
GO:0007268: synaptic transmission	**BP**	**2.19**	**40**	**13%**	$\mathbf{6 \times 10^{-6}}$	**0.003**
GO:0007267: cell–cell signaling	BP	2.16	86	13%	2×10^{-11}	9×10^{-8}
GO:0022610: biological adhesion	BP	2.10	98	13%	2×10^{-12}	10^{-8}
GO:0007155: cell adhesion	BP	2.10	98	13%	2×10^{-12}	10^{-8}
GO:0007610: behavior	BP	2.08	41	13%	2×10^{-5}	0.08
GO:0009611: response to wounding	BP	2.04	53	12%	10^{-6}	0.006
GO:0009605: response to external stimulus	BP	1.96	76	12%	2×10^{-8}	10^{-4}
GO:0048731: system development	BP	1.93	204	12%	2×10^{-21}	9×10^{-18}
GO:0009653: anatomical structure morphogenesis	BP	1.83	125	11%	2×10^{-11}	10^{-7}
GO:0042221: response to chemical stimulus	BP	1.78	65	11%	7×10^{-6}	0.04
GO:0007275: multicellular organismal development	BP	1.77	250	11%	2×10^{-21}	8×10^{-18}
GO:0048856: anatomical structure development	BP	1.75	227	11%	8×10^{-19}	4×10^{-15}
GO:0006950: response to stress	BP	1.66	108	10%	2×10^{-7}	8×10^{-4}

GO term	Type	Enr	*n*	% Of total	*P*-value	*P*-value (Bonf.)
GO:0005509: calcium ion binding	MF	1.65	95	10%	10^{-6}	0.004
GO:0007399: nervous system development	**BP**	**1.64**	**77**	**10%**	**2×10^{-5}**	**0.09**
GO:0005102: receptor binding	MF	1.63	77	9%	3×10^{-5}	0.07
GO:0032501: multicellular organismal process	BP	1.58	357	9%	4×10^{-23}	2×10^{-19}
GO:0032502: developmental process	BP	1.55	305	9%	5×10^{-18}	3×10^{-14}
GO:0048519: negative regulation of biological process	BP	1.53	109	9%	6×10^{-6}	0.03
GO:0030154: cell differentiation	BP	1.52	168	9%	10^{-8}	7×10^{-5}
GO:0048869: cellular developmental process	BP	1.52	168	9%	10^{-8}	7×10^{-5}
GO:0007154: cell communication	BP	1.25	309	7%	4×10^{-6}	0.02
GO:0005515: protein binding	MF	1.21	508	7%	8×10^{-9}	2×10^{-5}

% Of total, percentage from number of all known genes annotated with the GO term; Bonf., Bonferroni correction for multiple testing; BP, biological process; Enr, enrichment; GO, gene ontology; MF, molecular function; *n*, number of genes with the GO term in the list of differentially expressed genes. Boldface entries indicate neuronal differentiation.